

Small Molecule Interactions with Protein–Tyrosine Phosphatase PTP1B and Their Use in Inhibitor Design[†]

Terrence R. Burke, Jr.,^{*,‡} Bin Ye,[‡] Xinjian Yan,[‡] Shaomeng Wang,[‡] Zongchao Jia,[§] Li Chen,^{||} Zhong-Yin Zhang,^{||} and David Barford[§]

Laboratory of Medicinal Chemistry, Division of Basic Sciences, National Cancer Institute, National Institutes of Health, Bethesda, Maryland 20892, Laboratory of Molecular Biophysics, University of Oxford, South Parks Road, Oxford, England, and Department of Molecular Pharmacology, Albert Einstein College of Medicine, Bronx, New York 10461

Received May 28, 1996; Revised Manuscript Received September 27, 1996[®]

ABSTRACT: We have previously shown that a small peptide bearing the hydrolytically stable phosphotyrosyl (pTyr) mimetic, (difluorophosphonomethyl)phenylalanine (F₂Pmp), is an extremely potent inhibitor of PTP1B, with an IC₅₀ value of 100 nM [Burke, T. R., Kole, H. K., & Roller, P. P. (1994) *Biochem. Biophys. Res. Commun.* 204, 129–134]. We further demonstrated that removal of the peptide portion and incorporation of the difluorophosphonomethyl moiety onto a naphthalene ring system, but not a phenyl ring system, resulted in good inhibitory potency [Kole, H. K., Smyth, M. S., Russ, P. L., & Burke, T. R., Jr. (1995) *Biochem. J.* 311, 1025–1031]. In order to understand the structural basis for this inhibition, and to aid in the design of further analogs, we solved the X-ray structure of [1,1-difluoro-1-(2-naphthalenyl)-methyl]phosphonic acid (**6**) complexed within the catalytic site of PTP1B, solved to 2.3 Å resolution. In addition to showing the manner in which the phosphonate group is held within the catalytic site, the X-ray structure also revealed extensive hydrophobic interactions with the naphthalene ring system, beyond that possible with an analog bearing a single phenyl ring. It is further evident that, of the two fluorine atoms, the *pro-R* α-fluorine interacts with the enzyme to a significantly greater degree than the *pro-S* α-fluorine, forming a hydrogen bond to Phe 182. On the basis of a computer-assisted molecular modeling analysis, it was determined that addition of a hydroxyl to the naphthyl 4-position, giving [1,1-difluoro-1-[2-(4-hydroxynaphthalenyl)]methyl]phosphonic acid (**8**), could potentially replace a water molecule situated in the PTP1B·**6** complex, thereby allowing new hydrogen-bonding interactions with Lys 120 and Tyr 46. Compound **8** was therefore prepared and found to exhibit a doubling of affinity (*K*_i = 94 μM) relative to parent unsubstituted **6** (*K*_i = 179 μM), supporting, in principle, the development of high-affinity ligands based on molecular modeling analysis of the enzyme-bound parent.

Kinase-dependent signaling pathways are central mediators of cellular physiology and afford new targets for the development of a variety of therapeutics. Protein–tyrosine kinase (PTK) mediated phosphorylation of tyrosyl residues within specific signaling proteins generates “phosphotyrosyl (pTyr, 1; Figure 1) motifs” which act as molecular switches, modulating the flow of signaling information. In this scheme, protein–tyrosine phosphatases (Stone & Dixon, 1994) (PTPs) act in partnership with PTKs to control signaling by maintaining tyrosyl residues in their proper phosphorylation states, with the action of PTPs manifesting either positive or negative regulation on the signaling process (Hunter, 1995; Sun & Tonks, 1994). Although PTP inhibitors have potential value both as pharmacologic tools and

as therapeutic agents, little has been reported on their development (Berggren et al., 1993; Cao et al., 1995; Caselli et al., 1994; Errasfa & Stern, 1993; Ghosh & Miller, 1993; Horiguchi et al., 1994; Imoto et al., 1993; Miski et al., 1995; Posner et al., 1994; Wang et al., 1994; Watanabe et al., 1994). One reason for this may be a less than clear understanding of the structural requirements for inhibitor design. We have therefore undertaken the stepwise design and synthesis of PTP inhibitors through the use of nonhydrolyzable pTyr mimics which can function as competitive inhibitors at the PTP catalytic site. Relying on studies which showed that peptides containing the pTyr mimic 4-(phosphonomethyl)phenylalanine (Pmp, **2**) are effective PTP inhibitors (Chatterjee et al., 1992; Zhang et al., 1994), we previously prepared a Pmp-containing hexamer peptide based on the epidermal growth factor receptor-derived sequence (EGFR_{988–993}), “D-A-D-E-X-L”, where X = Tyr, which has been shown to be a good PTP substrate when X = pTyr (Zhang et al., 1994). The resulting peptide, “Ac-D-A-D-E-X-L-amide”, where X = Pmp was compared to the same peptide containing (difluorophosphonomethyl)phenylalanine (F₂Pmp, **3**), which is a Pmp analogue having two fluorines substituted at the phosphonate α-methylene (Burke et al., 1993a,b; Smyth & Burke, 1994). It was found that the F₂Pmp-containing peptide exhibited a 1000-fold enhancement in PTP binding relative to its Pmp counterpart (Burke et al.,

[†] A preliminary account of this work has been reported: Burke, T. R., Jr., Kole, H. K., Yan, X., Barford, D., & Ye, B. (1995) Third Chemical Congress of the Pacific Basin Societies, Honolulu, HI, Dec 17–22, abstract ORGN 1397. This work was supported in part by a grant from the National Institutes of Health, DRTC 5P60 DK20541, to Z.-Y.Z., by a grant from the Wellcome Trust (042552/Z/94/Z to D.B.), and by a Natural Sciences and Engineering Research Council of Canada Grant to Z.J.

^{*} To whom correspondence should be addressed at the Laboratory of Medicinal Chemistry, National Cancer Institute, Building 37, Room 5C06, National Institutes of Health, Bethesda, MD 20892.

[‡] Laboratory of Medicinal Chemistry, NCI.

[§] University of Oxford.

^{||} Albert Einstein College of Medicine.

[®] Abstract published in *Advance ACS Abstracts*, November 15, 1996.

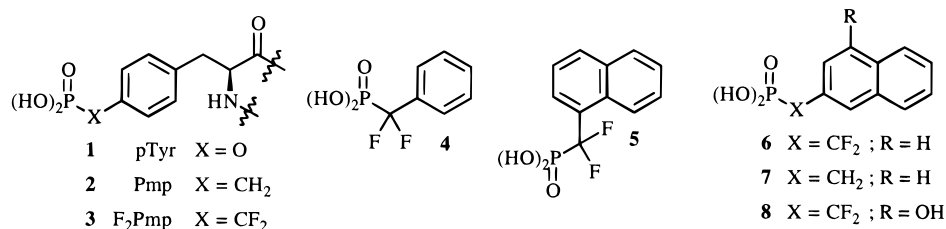


FIGURE 1: Structures of pTyr mimics and related inhibitors.

1994a). This provided the first indication that the difluorophosphonate pharmacophore can contribute to high PTP binding affinity. We subsequently examined small difluorophosphonate-containing molecules lacking a peptide component and showed that while the simplest aryl-containing analog, (α,α -difluorobenzyl)phosphonic acid (**4**), had little affinity, adding a second phenyl ring to provide the corresponding 1- or 2-substituted [(1,1-difluoro-1-naphthalenyl)methyl]phosphonic acids (**5** and **6**, respectively) gave good binding potency (Burke et al., 1994b; Kole et al., 1995). As seen previously with the peptide-based inhibitors, the fluorines played an important role in the binding interaction, since the corresponding nonfluorinated [(2-naphthalenyl)methyl]phosphonic acid (**7**) had no measurable binding. In further studies we have recently shown that the fluorines may enhance PTP binding affinity by interacting with the enzyme directly (Chen et al., 1995), rather than by some secondary mechanism such as lowering phosphonate pK_a values, as seen with SH2 domain binding (Burke et al., 1994c; Smyth et al., 1992).

The [1,1-difluoro-1-(2-naphthalenyl)methyl]phosphonic acid (**6**) therefore provides a starting nucleus from which more potent small molecules can potentially be developed. In order to facilitate the rational design of new analogs, it was important to determine the nature of the binding interactions between **6** and the PTP catalytic site. Such information could have broad implications for understanding the way small molecules interact with the catalytic site. In the present work we have therefore obtained the X-ray crystallographic structure of **6** bound within the catalytic cavity of the human protein-tyrosine phosphatase 1B (PTP1B). This enzyme was the first PTP to have its structure solved by X-ray (Barford et al., 1994a). On the basis of the X-ray structure of the complex between PTP1B and **6**, the orientation within the catalytic site of both the difluorophosphonate moiety and the naphthyl ring system to which it was attached became evident. Analysis of these binding interactions indicated that introduction of a hydroxyl at the naphthyl 4-position could enhance binding interactions. We herein report the X-ray structure of the **6**•PTP1B complex and detail molecular modeling considerations which lead to the design of inhibitor **8** as well as their potential application for the design of further small molecule inhibitors. We also report the kinetic evaluation of **8** and interpret these data in light of molecular modeling-derived energetics.

MATERIALS AND METHODS

X-ray Crystallography. The N-terminal 321 residues of the mutant PTP1B (Cys 215 \rightarrow Ser) were purified and crystallized as reported previously (Barford et al., 1994b; Jia et al., 1995). Crystals of PTP1B were soaked in a solution containing 5 mM [1,1-difluoro-1-(2-naphthalenyl)methyl]phosphonic acid (**6**), 0.1 M Hepes (pH 7.5), 0.2 M

magnesium acetate, and 13% (w/v) poly(ethylene glycol) 8000 for 1 h, prior to soaking in an identical solution with increasing concentrations of glycerol to a final concentration of 25% (v/v) and freezing at 100 K. X-ray crystallographic data were collected to a resolution of 2.3 Å at station PX 9.5, SRS, Daresbury, U.K., using an 18 cm MAR imaging plate from a single crystal at 100 K. Data processing and reduction were performed using DENZO and SCALEPACK. Finally the data were processed using TRUNCATE (French & Wilson, 1978). The model of PTP1B (Barford et al., 1994b) was refined against crystallographic data using X-PLOR (Brunger, 1992) using Engh and Huber parameters (Engh & Huber, 1991). The resultant preliminary refined model was used to calculate $2F_o - F_c$ and $F_o - F_c$ difference electron density maps. The density arising from **6** located at the catalytic site was easily interpretable, and a model for **6** was fit to the electron density maps using the program O (Jones et al., 1991). This complex was subjected to further refinement with X-PLOR. Superimpositions of the PTP1B•pTyr (Jia et al., 1995) and PTP1B•**6** complexes were performed using SUPERSIEVE (Barford et al., 1988).

Molecular Modeling. The atomic charges for compounds **6** and **8** were calculated using GAUSSIAN 92 with a 3-21g* basis set. All simulations were performed using the CHARMM program (version 24), with all-atom parameters (version 22 as supplied by Molecular Simulations, Inc.). The X-ray structure of PTP1B•**6** was used as the starting structure for subsequent simulations of this complex. Starting from the X-ray structure of bound **6**, compound **8** was constructed using QUANTA and then docked into the catalytic site of PTP1B in a manner similar to that observed in the parent PTP1B•**6** complex. This complex was then used as the starting point for all PTP1B•**8** calculations.

Simulations were performed by hydrating the system with 1100 TIP3P water molecules in the case of enzyme-inhibitor complexes and 300 TIP3P water molecules for systems having inhibitors only. The hydrated systems were minimized first by constraining the protein and inhibitors for 2000 iterations using an Adjusted Basis Newton-Raphson algorithm, as implemented in the CHARMM program. The constraints were released, and the whole system was then minimized with 5000 iterations or until convergence (defined as an energy gradient of 0.001 kcal mol⁻¹ Å⁻¹ or less). The hydrated systems were heated from 0 to 300 K in 10 ps and equilibrated for 20 ps. The complexes and inhibitors were then simulated for 100 or 200 ps, respectively. During the simulations, trajectories were recorded every 0.1 ps and were subsequently analyzed. The cutoff distance for nonbonding interactions was set at 14 Å. A switched potential was used for the van der Waals interactions, and a shifted function was applied to the electrostatic interactions. The cutoff distance for force was set at 12 Å, and a switched potential function was used for force evaluations.

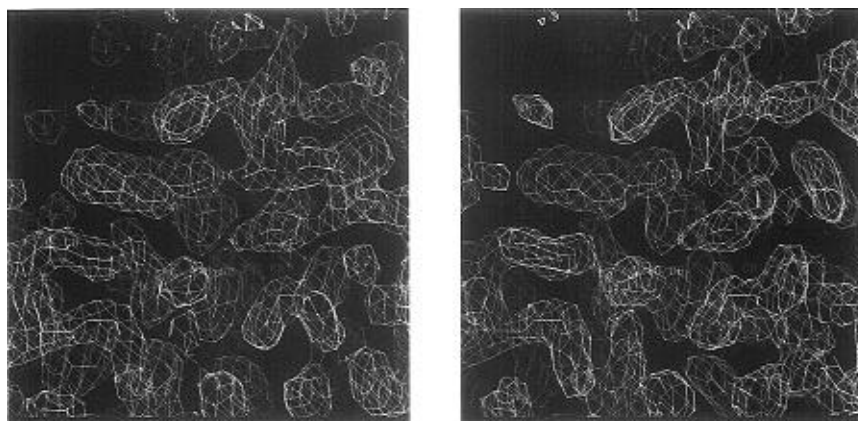


FIGURE 2: View of a $2F_o - F_c$ electron density map of the PTP1B·6 complex in the vicinity of the catalytic site. Figure produced using O (Jones et al., 1991).

Synthesis of Inhibitor 8. Although structurally similar to the previously reported unsubstituted parent **6** (Smyth et al., 1992), inhibitor **8** proved significantly more challenging to synthesize and was prepared in 12 steps from commercially available 1,3-dihydroxynaphthalene (Ye & Burke, 1996). The synthesis required initial differential protection of the 1-hydroxyl group as its tosyl ester, followed by palladium-mediated carbonylation of the suitably activated 3-hydroxyl group to yield the 3-methyl carboxylate. The ester functionality was then transformed into the difluorophosphonate group using previously published procedures (Smyth et al., 1992).

Biological. (A) Recombinant Enzymes. The recombinant catalytic domain of mammalian protein-tyrosine phosphatase 1 (PTP1) was created by inserting a stop codon at residue 323, yielding PTP1U323, in order to eliminate the hydrophobic membrane "targeting" domain of the molecule. Homogeneous recombinant catalytic domain PTP1U323, from here on referred to PTP1, was purified as described (Hengge et al., 1995).

(B) Enzyme Assay. The PTPase activity was assayed at 30 °C in a reaction mixture (0.2 mL) containing appropriate concentrations of *p*-nitrophenyl phosphate as substrate. The buffer used was pH 7.0, 50 mM 3,3-dimethylglutarate and 1 mM EDTA. The ionic strength of the solution was kept at 0.15 M using NaCl. The reaction was initiated by addition of PTP1 and quenched after 2–3 min by addition of 1 mL of 1 N NaOH. The nonenzymatic hydrolysis of the substrate was corrected by measuring the control without the addition of enzyme. The amount of product *p*-nitrophenol was determined from the absorbance at 405 nm using a molar extinction coefficient of 18 000 M⁻¹ cm⁻¹. Michaelis–Menten kinetic parameters were determined from a direct fit of the v vs $[S]$ data to the Michaelis–Menten equation using the nonlinear regression program GraFit (Erithacus Software).

(C) Determination of K_i Values. Inhibition constants for **5**, **6**, and **8** were determined for homogeneous PTP1 in the following manner. At various fixed concentrations of inhibitors (0, 100, and 300 μ M), the initial rate at eight different *p*-nitrophenyl phosphate concentrations (0.2 K_m to 5 K_m) was measured as described (Zhang, 1995). The data were fit to the equation $v = V_{max}S/(K_m[1 + K_i] + S)$ using KINETASYST (IntelliKinetics, State College, PA) to obtain the inhibition constant (K_i).

Table 1: Results of Crystal Structure Determination of the PTP1B·[1,1-Difluoro-1-(2-naphthalenyl)methyl]phosphonic Acid Complex

Crystal Parameters	
space group	<i>P</i> 3 ₁ 21
<i>a</i>	88.4 Å
<i>b</i>	88.4 Å
<i>c</i>	104.0 Å
Data Collection and Processing Statistics	
X-ray source	PX 9.5 SRS, Daresbury
resolution	2.3 Å
R_{sym}^a	0.090
no. of observations	116577
no. unique reflections (% complete)	20894 (97.4)
Refinement Statistics	
resolution	8.0–2.3 Å
no. of reflections	20466
no. of protein and ligand atoms	2449
no. of water molecules	266
<i>R</i> factor ^b	0.195
rmsd ^c bond lengths	0.007
rmsd ^c bond angles	1.377
rmsd ^c dihedrals	23.373
rmsd ^c improvers	1.184

^a $R_{sym} = \sum_i \sum_h |I_i(h) - I_i(h)| / \sum_i \sum_h I_i(h)$, where $I_i(h)$ and $I(h)$ are the *i*th and the mean measurements of the intensity of reflection *h*. ^b *R* factor = $\sum_h |F_o - F_c| / \sum_h F_o$, where F_o and F_c are the observed and calculated structure factor amplitudes of reflection *h*. ^c rmsd = root mean square deviation from ideality.

RESULTS AND DISCUSSION

X-ray Crystallography. The $2F_o - F_c$ electron density map in the vicinity of the catalytic site including the density corresponding to [1,1-difluoro-1-(2-naphthalenyl)methyl]phosphonic acid (**6**) is shown in Figure 2. The structure of **6** is clearly defined within the electron density maps with, for example, well-resolved density for the fluorine atoms on the phosphonate group. All protein residues from 1 to 298 are defined in the electron density map, and the structure has been refined to an *R* factor of 0.18 (Table 1). The structures of PTP1B in complex with pTyr (Jia et al., 1995) and **6** are very similar (Figure 3). Overall, all atoms superimpose to within a root mean square deviation of 0.95 Å, and 79.5% of atoms superimpose within a rms deviation of 0.3 Å. [1,1-Difluoro-1-(2-naphthalenyl)methyl]phosphonic acid (**6**) binds to the catalytic site of PTP1B in a fashion similar to that of pTyr bound to PTP1B (Jia et al., 1995) (Figures 3 and 4). Specifically, the phosphate groups of pTyr and **6** superimpose as does the phenyl ring of pTyr with the

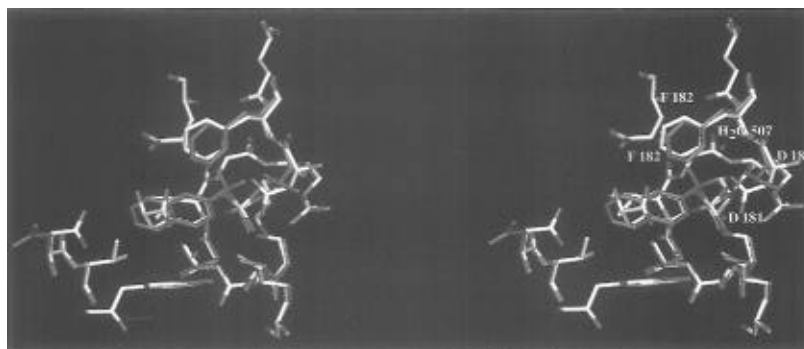


FIGURE 3: Stereo superimposition of the refined coordinates of PTP1B•6 (purple) and PTP1B•pTyr (white).

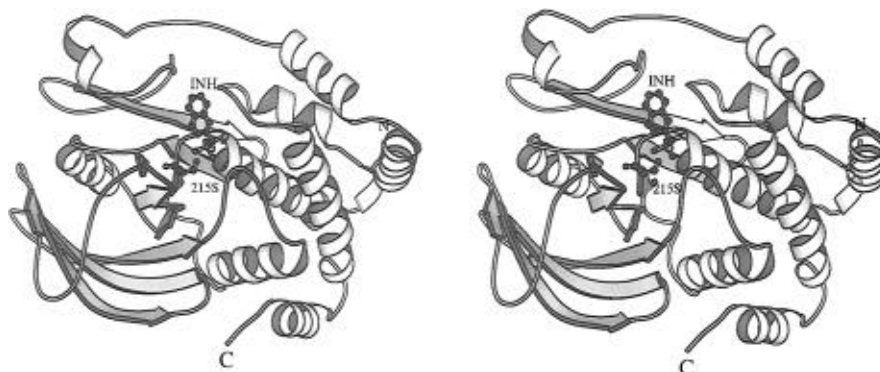


FIGURE 4: Ribbon figure of PTP1B with [1,1-difluoro-1-(2-naphthalenyl)methyl]phosphonic acid (**6**) bound at the catalytic site. The side chain of Ser 215 is shown. Figure produced using MOLSCRIPT and is shown in stereo (Kraulis, 1991).

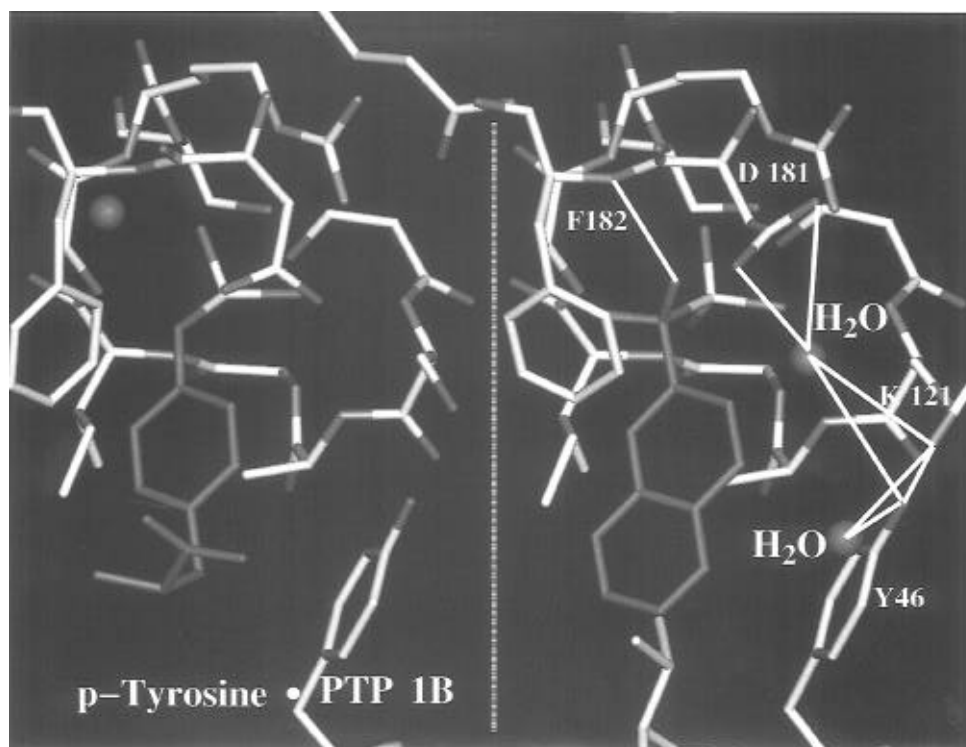


FIGURE 5: Catalytic site of PTP1B bearing a pTyr residue (left; Jia et al., 1995) and [1,1-difluoro-1-(2-naphthalenyl)methyl]phosphonic acid (**6**) (right). Relevant H₂O molecules are shown as red spheres, with key H-bond interactions depicted using white lines.

first six-membered ring of **6**. Binding of **6** to PTP1B induces motion of a loop consisting of Trp 179 to Ser 187, similar to that observed for the binding of pTyr to PTP1B. However, notable differences in conformation of the side chains of Asp 181 and Phe 182 are observed as a result of the two fluorine atoms located on the phosphonate carbon atom of **6**. In addition, a buried water molecule observed in the PTP1B•

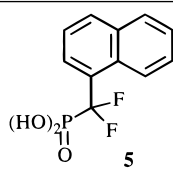
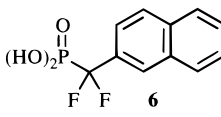
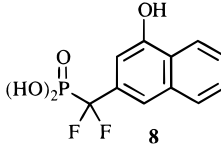
pTyr complex located between the main-chain NH of Phe 182 and the scissile oxygen of pTyr is absent in the PTP1B•**6** complex (Figure 5). In the PTP1B•pTyr complex, the side chain of Asp 181 forms a H-bond with the buried water molecule and a long contact (3.5 Å) with the scissile oxygen of PTP1B. The two fluorine atoms on **6** partially occupy the water binding site, causing displacement of the water

molecule and a shift in position of the side chain of Asp 181 to avoid close contact with one of the fluorine atoms (3.2 Å without motion of Asp 181). Concerted with the motion of the side chain of Asp 181 is a rotation of the side chain of Phe 182 by 60° about the C_β–C_γ bond (Figure 3) caused in part to avoid close contact between the CD2 atom of Phe 182 and F1 of **6**. In the resultant PTP1B•**6** structure, the phenyl ring of Phe 182 forms van der Waals contacts with the two fluorine atoms of **6** with CE1 and CE2 of Phe 182 3.6 and 3.7 Å from F1 and F2 of **6**, respectively (Figure 3). The naphthalene-2-difluorophosphonic acid moiety is located within an amphipathic pocket of PTP1B with its phosphate group forming hydrogen bonds to main chain nitrogens of residues Ser 215 to Arg 221 and, in addition, two salt bridges with the guanidinium side chain of Arg 221. The naphthalene ring of the inhibitor forms hydrophobic interactions with the side chains of Tyr 46, Phe 182, Ala 217, Ile 219, and the nonpolar groups of Gln 262 (Figure 3).

Design of Inhibitor 8. It is observed that two water molecules (designated as H₂O 301 and H₂O 617) bind to residues Tyr 46, Lys 120, and Asp 181 in the enzyme–inhibitor complex (Figure 5). The positioning of these water residues situates them in close proximity to the naphthalene ring system. It became apparent that addition of a hydroxyl group to either the C3 or C4 positions of the naphthalene ring in parent **6** could potentially mimic one of these water molecules. Such a modification could enhance binding affinity through entropic considerations. Although the hydroxyl group could be attached at either the C3 or C4 positions in **6**, the C4 position seemed a better choice, since the combined distance to the oxygen atoms of H₂O 617 (3.4 Å) and H₂O 301 (4.0 Å) was less than the corresponding distance between a C3-situated hydroxyl and the same oxygens (3.2 and 5.1 Å, respectively). In the resulting new inhibitor **8**, the hydroxyl situated at the C4 position would, in essence, mimic both water molecules, although only in an approximate manner. Since displacement of the original water molecules is not exact, side chain deformations of the Tyr 46, Lys 120, and Asp 18 would be expected, which could potentially incur energy penalties.

Kinetic Analysis. The inhibition constants for 1- and 2-substituted [(1,1-difluoro-1-naphthalenyl)methyl]phosphonic acids (**5** and **6**) were determined against the mammalian PTP1. PTP1 (Guan et al., 1990) is the rat homolog of the human PTP1B. The catalytic domain of PTP1 resides between residues 1 and 322 and is 97% identical to the corresponding 322 residues of the human PTP1B. It was found that both **5** and **6** are competitive inhibitors of PTP1 using *p*-nitrophenyl phosphate as a substrate (data not shown) with *K*_i values of 255 and 179 μM, respectively, at pH 7.0 (Table 2). This is a surprising result, since we have previously shown that α-naphthyl phosphate is a much poorer substrate than β-naphthyl phosphate, primarily due to a decrease in the *k*_{cat} value (Zhang, 1995). Since PTP catalysis is nucleophilic in nature (Zhang & Dixon, 1994), it is understandable that the unfavorable steric hindrance in α-naphthyl phosphate is detrimental to catalysis. The fact that **5** and **6** display comparable inhibition constants indicates that the active site of PTP1 is flexible in accommodating different substituted naphthalenylphosphonic acids. Alternatively, compounds **5** and **6** may adapt different conformations in the active site. The prediction, based on molecular

Table 2: Inhibition Constants Determined for Indicated Inhibitors against PTP1 As Indicated in Materials and Methods

compound	<i>K</i> _i (μM)
	255 ± 18
	179 ± 25
	93 ± 8

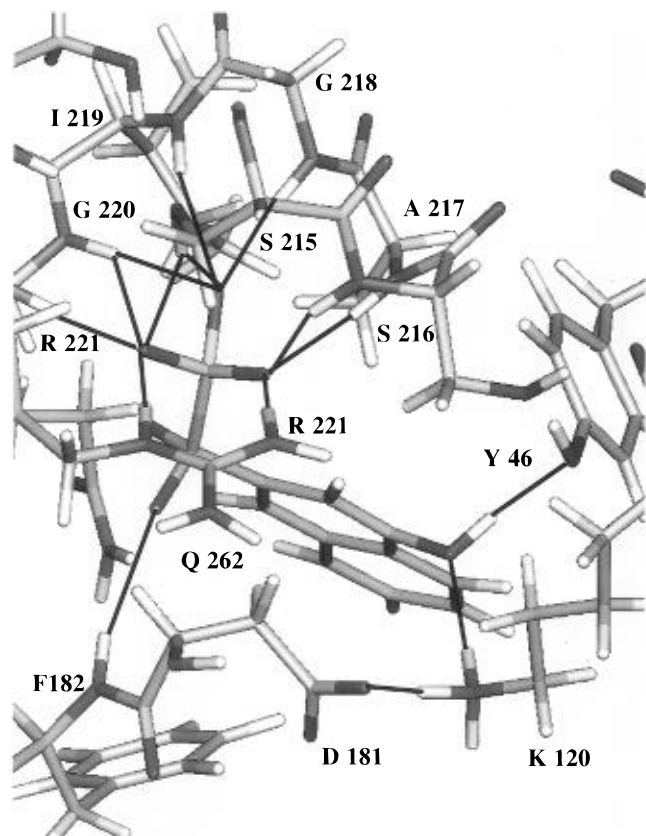
modeling (see below), that addition of a hydroxyl group to the 4-position of the naphthalene ring, to provide **8**, should enhance binding interaction was borne out, as the inhibition constant for **8** was determined to be 93 μM (Table 2). This value is 2-fold lower than that of unhydroxylated parent **6**.

Molecular Modeling Studies. The X-ray structure of PTP1B•**6** provided the structural basis for the design of new inhibitors with improved affinity. As described above, a number of X-ray crystallographic water molecules were found adjacent to **6** tightly bound to the enzyme. In principle, incorporation of water molecules into an inhibitor could potentially improve binding affinity by displacing and releasing these tightly bound water molecules, resulting in an increase in the entropy of the system. Indeed, such design strategy has led to the successful development of a class of highly potent, nonpeptidic HIV protease inhibitors (Lam, 1994). Through analysis of the X-ray structure of PTP1B•**6**, it became evident that a hydroxyl group at the C-4 position of the naphthalene ring (compound **8**) could potentially mimic and thus replace two crystallographic water molecules (H₂O 301 and 617). To confirm this observation, **8** was docked into the binding site of PTP1B in a binding mode similar to that of **6**. The structures of the resulting complexes, PTP1B•**6** and PTP1B•**8** were then subjected to energy minimization and 100 ps molecular dynamics simulations at 300 K, solvated using 1100 TIP3P water molecules.

Analysis of 100 molecular dynamics simulation trajectories showed that, indeed, the additional C-4 hydroxyl group in **8** resulted in an increase of −19.1 kcal/mol in interaction energy between **8** and the enzyme, as compared to the unhydroxylated **6** (−299.9 versus −280.8 kcal/mol, Table 3). As shown in Figure 6, this increase in interaction energy is primarily due to the formation of two new strong hydrogen bonds between the C-4 hydroxyl in our calculated binding model for **8** and Tyr 46 and Lys 120. Our analysis also showed that formation of these new hydrogen bonds induced changes in the side chain conformations of Tyr 46, Lys 120, and Asp 181, resulting in a calculated conformational energy penalty of 7.7 kcal/mol on average over the simulation interval. The conformational energy penalty is, however, smaller than the increase of the interaction energy of −19.1 kcal/mol for **8**, suggesting that the additional hydroxyl group may be advantageous and that **8** should exhibit increased

Table 3: Analysis of Molecular Dynamics Simulation Trajectories of Inhibitors **6** and **8** While Complexed to PTP1B

	6 (kcal/mol)	8 (kcal/mol)
total interaction energy with enzyme	-280.8 ± 9.8	-299.9 ± 8.6
total electrostatic energy with enzyme	-261.0 ± 9.7	-280.7 ± 8.5
total van der Waals interaction energy with enzyme	-20.3 ± 2.9	-19.3 ± 2.8
total interaction energy with water molecules in complex	-43.5 ± 6.9	-38.7 ± 6.7
total interaction energy with both enzyme and solvent in complex	-324.4 ± 10.0	-338.6 ± 9.2
total interaction energy with solvent when solvated	-348.8 ± 15.4	-343.5 ± 14.7
interaction energy of the phosphonate group with enzyme	-201.9 ± 6.6	-198.7 ± 5.9
interaction energy of the phosphonate group with solvent when solvated	-202.6 ± 10.5	-195.9 ± 12.6

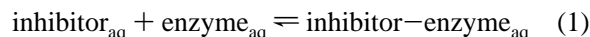
FIGURE 6: Molecular simulation of PTP1B complexed with [1,1-difluoro-1-(2-(4-hydroxynaphthalenyl)methyl)phosphonic acid (**8**) performed as indicated in Materials and Methods.

potency. This prediction was confirmed experimentally by a 2-fold enhancement in the K_i value for **8** as compared with parent **6**.

To more clearly elucidate the nature of the interactions between these inhibitors and the enzyme, we have partitioned the total interaction energy into electrostatic and van der Waals energy terms using the CHARMM energy function and its associated parameter set. As can be seen from Table 3, van der Waals energy was only 7.2% and 6.4% of the total for **6** and **8**, respectively, while the electrostatic energy term accounts for the remaining 92.8% and 93.6%. This indicates that the binding interactions for both inhibitors are primarily electrostatic in nature. These results are expected since under physiological conditions both **6** and **8** are deprotonated. The resulting -2 charge is largely localized to the phosphonate moiety which interacts with the highly

positively charged phosphate binding region (Figure 6). It is also of note that, in their complexed forms, both **6** and **8** are partially exposed to solvent, as is evidenced from the significant interaction energy with the solvent (Table 3).

It is somewhat surprising that the large interaction energy between the inhibitors and the enzyme does not result in extremely tight binding ($K_i = 179 \mu\text{M}$ and $93 \mu\text{M}$ for **6** and **8**, respectively; Table 2). To understand this, it is worthwhile to consider the binding process:



The binding affinity is determined by the change in free energy as described by (1) using the equation, $\Delta G = 2.303RT \log K_i$. This depends not only on the interaction between the inhibitor and the enzyme but also on the solvation energies of both the enzyme and the inhibitor, as well as entropic changes associated with binding. To better understand the role in the binding process played by solvation of the inhibitor, we carried out 200 ps molecular dynamics simulations of both **6** and **8** at 300 K, solvated by 300 TIP3P water molecules. Analysis of trajectories showed that the average interaction energy between the inhibitor and solvent molecules (water) is -348.8 and -343.5 kcal/mol for **6** and **8**, respectively (Table 3). These values are somewhat larger than the total interaction energies for **6** and **8** when binding to the enzyme. Since these large interaction energies are predominantly due to the phosphonate group, we evaluated its contribution to the total interaction energy with the inhibitor both solvated in water and bound to the enzyme. It was found that the phosphonate group in **6** contributes on average -201.9 kcal/mol to the enzyme-inhibitor interaction and -202.6 kcal/mol to solvation, while for **8**, -198.7 kcal/mol for the enzyme-inhibitor interaction and -195.9 kcal/mol for the solvation were observed (Table 3). Therefore, the net gain in interaction energy from the phosphonate group (presumably the enthalpy term) when transferring inhibitor from a solvent environment to the enzyme is 0.7 and -2.8 kcal/mol for **6** and **8**, respectively. Although these results depend upon the molecular mechanics parameters employed in the calculations and should be treated with caution, they do suggest that the highly charged phosphonate group may contribute very little to the total enthalpy of binding between the enzyme and the inhibitors. The role played by the phosphonate group in the binding may be 2-fold. First, since the enzyme possesses a partially positively charged binding pocket, the negatively charged phosphonate group may be important for enzyme-inhibitor recognition. Second, binding of the phosphonate group to enzyme displaces water molecules originally occupying the binding site, thus providing entropic gain. In this latter case, groups similar in size but less negatively charged may be employed to replace the phosphonate group. Such a modification may result in new inhibitors with improved cellular penetration.

It is also of note that, in both the X-ray structure of PTP1B•**6** and our calculated PTP1B•**8** complex, an unconventional hydrogen bond exists between one of the fluorine atoms and the amido group of Phe 182. This hydrogen bond was maintained throughout the entire molecular dynamics simulations and probably plays an important role for enhancing the binding affinities of **6** and **8**, since **7**, which lacks fluorines, has little binding affinity to the enzyme (Kole et al., 1995). Additionally, although the phosphonate

α -methylene bears two fluorine atoms, only the *pro-R* fluorine forms a hydrogen bond with the enzyme. Indeed, our calculations indicate that the *pro-R* fluorine contributes an average of -4.6 kcal/mol more interaction energy than the *pro-S* fluorine when binding to the enzyme, while both fluorine atoms have a similar interaction energy with the solvent when these inhibitors are entirely solvated by water molecules.

Implications for Inhibitor Design. Previously we had demonstrated that small substrate-based peptides containing the nonhydrolyzable pTyr mimetic F₂Pmp (**3**) showed extremely high affinity for PTPs (Burke et al., 1994a). In further studies we also showed that nonpeptidic, small molecule arylmethylphosphonates can also be effective PTP inhibitors, provided they contain both the difluorophosphonomethyl and naphthyl functionalities (Kole et al., 1995). The present study has clarified the structural basis for these dual requirements. One result of this work is that a chiral monofluorophosphonate may bind with good affinity relative to its difluoro counterpart. The slight elevation in the phosphonate pK_{a2} value in going from the difluoro to the monofluoro species [anticipated to be approximately 0.5 pK_a unit (Smyth et al., 1992)] would not be expected to adversely affect affinity, since we have also shown a lack of pH dependence for binding of the parent analog **6** (Chen et al., 1995).

The X-ray structure of the PTP1B•**6** complex shows that binding interactions occur with the second aryl ring of the bis(aryl)naphthalene nucleus, that are not found in compounds possessing a single aryl ring, such as phenyl phosphate. This supports both our previous observation that the difluorophosphonomethylphenyl compound **4** had little affinity, while the corresponding naphthyl derivatives **5** and **6** exhibited good affinities (Kole et al., 1995). Multiple binding interactions appear possible for polyaromatic systems. This is suggested both by the X-ray structure of the PTP1B•**6** complex, and by the fact that shifting the position of the difluorophosphonomethyl group from the 2- to the 1-position of the naphthalene ring system (compounds **6** and **5**, respectively) did not drastically reduce affinity. Since the phosphonate moiety provides a tightly bound anchor within the catalytic cavity, altering its site of attachment to the naphthyl ring system would most probably dramatically affect the binding orientation of the ring system. The fact that this change did not significantly reduce affinity, strongly suggests great latitude in the use of polyaromatic ring systems within inhibitors.

The molecular dynamics results suggesting that the phosphonate group may enhance binding by occupying the binding pocket and displacing water molecules, thereby achieving a net entropy gain, present an exciting opportunity for the design of new PTP inhibitors. These data indicate that replacement of the phosphonate functionality with similarly sized uncharged species may be possible, provided that these replacements do not induce a significant loss in enthalpy when transferring from the aqueous to the protein phase. Interestingly, a recent report has appeared that certain aporphine alkaloids are inhibitors of the tyrosine phosphatase CD45 (Miski et al., 1995). While the mode of the binding interactions of these inhibitors with the CD45 was not indicated, the non-phosphonate-containing polyaromatic nature of these molecules is consistent with the types of structures allowed by our modeling.

In conclusion, this study has explored the ability to employ molecular modeling to "design in" recognition features which afford enhanced binding interactions. On the basis of modeling considerations, it was anticipated that addition of a hydroxyl to the naphthyl 4-position (compound **8**) should allow specific hydrogen bonds to elements within the catalytic site (Lys 120 and Tyr 46). The 2-fold enhancement in binding affinity achieved by **8** (Table 2) validates the principle that higher affinity ligands can be designed on the basis of modeling considerations of the enzyme-bound parent. Presently, due to a poor understanding of entropy changes involved in the binding process, it is not possible to assign quantitative predictions as to these relative binding affinities. Nonetheless, the approach utilized serves as a general procedure which allows semiquantitative predictions of changes in binding affinity which may result upon structural modifications to a reference inhibitor. Such an approach has predictive value in structure-based drug design. Finally, it should be mentioned that questions of selectivity among phosphatases were not addressed in our study. For example, we have previously demonstrated that compound **6** has good affinity for the serine/threonine phosphatase PP2A (Kole et al., 1995). Additional studies will be required to define structural criteria related to matters of specificity.

REFERENCES

- Barford, D., Schwabe, J. W. R., Oikonomakos, N. G., Acharya, K. R., Hajdu, J., Papageorgiou, A. C., Martin, J. C., Knott, J. C. A., Vasella, A., & Johnson, L. N. (1988) *Biochemistry* 27, 6733–6741.
- Barford, D., Flint, A. J., & Tonks, N. K. (1994a) *Science* 263, 1397–1404.
- Barford, D., Keller, J. C., Flint, A. J., & Tonks, N. K. (1994b) *J. Mol. Biol.* 239, 726–730.
- Bell, K. H., & McCaffery, L. F. (1993) *Aust. J. Chem.* 46, 731–737.
- Berggren, M. M., Burns, L. A., Abraham, R. T., & Powis, G. (1993) *Cancer Res.* 53, 1862–1866.
- Brunger, A. T. (1992) *X-PLOR: version 3.1; a system for protein crystallography and NMR*, Yale University Press, New Haven, CT.
- Burke, T. R., Jr., Smyth, M., Nomizu, M., Otaka, A., & Roller, P. P. (1993a) *J. Org. Chem.* 58, 1336–1340.
- Burke, T. R., Smyth, M. S., Otaka, A., & Roller, P. P. (1993b) *Tetrahedron Lett.* 34, 4125–4128.
- Burke, T. R., Jr., Kole, H. K., & Roller, P. P. (1994a) *Biochem. Biophys. Res. Commun.* 204, 129–134.
- Burke, T. R., Jr., Smyth, M. S., & Kole, H. K. (1994b) 208th National Meeting of the American Chemical Society, Washington, DC, Abstract MEDI 46.
- Burke, T. R., Jr., Smyth, M. S., Otaka, A., Nomizu, M., Roller, P. P., Wolf, G., Case, R., & Shoelson, S. E. (1994c) *Biochemistry* 33, 6490–6494.
- Cacchi, S., Ciattini, G. P., Morera, E., & Ortar, G. (1986) *Tetrahedron Lett.* 27, 3931–3934.
- Cao, X. D., Moran, E. J., Siev, D., Lio, A., Ohashi, C., & Mjalli, A. M. M. (1995) *Bioorg. Med. Chem. Lett.* 5, 2953–2958.
- Caselli, A., Camici, G., Manao, G., Moneti, G., Pazzagli, L., Cappugi, G., & Ramponi, G. (1994) *J. Biol. Chem.* 269, 24878–24882.
- Chatterjee, S., Goldstein, B. J., Csermely, P., & Shoelson, S. E. (1992) in *Peptides: Chemistry and Biology* (Rivier, J. E., & Smith, J. A., Eds.) pp 553–555, Escom Science Publishers, Leiden, The Netherlands.
- Chen, L., Wu, L., Otaka, A., Smyth, M. S., Roller, P. P., Burke, T. R., Denhartog, J., & Zhang, Z. Y. (1995) *Biochem. Biophys. Res. Commun.* 216, 976–984.
- Engh, R. A., & Huber, R. (1991) *Acta Crystallogr.* A47, 392–400.
- Errasfa, M., & Stern, A. (1993) *Eur. J. Pharmacol.* 247, 73–80.

- Ghosh, J., & Miller, R. A. (1993) *Biochem. Biophys. Res. Commun.* 194, 36–44.
- Griffiths, D. V., Griffiths, P. A., Whitehead, B. J., & Tebby, J. C. (1992) *J. Chem. Soc., Perkin Trans. 1*, 479–484.
- Guan, K. L., Haun, R. S., Watson, S. J., Geahlen, R. L., & Dixon, J. E. (1990) *Proc. Natl. Acad. Sci. U.S.A.* 87, 1501–1505.
- Hengge, A. C., Sowa, G. A., Wu, L., & Zhang, Z. Y. (1995) *Biochemistry* 34, 13982–13987.
- Horiguchi, T., Nishi, K., Hakoda, S., Tanida, S., Nagata, A., & Okayama, H. (1994) *Biochem. Pharmacol.* 48, 2139–2141.
- Hunter, T. (1995) *Cell* 80, 225–236.
- Imoto, M., Kakeya, H., Sawa, T., Hayashi, C., Hamada, M., Takeuchi, T., & Umezawa, K. (1993) *J. Antibiot.* 46, 1342–1346.
- Jia, Z., Barford, D., Flint, A. J., & Tonks, N. K. (1995) *Science* 268, 1754–1758.
- Jones, T. A., Zou, J.-Y., Cowan, S. W., & Kjeldgaard, M. (1991) *Acta Crystallogr.* A47, 110–119.
- Jung, M. E., & Lazarova, T. I. (1996) *Tetrahedron Lett.* 37, 7–8.
- Kole, H. K., Smyth, M. S., Russ, P. L., & Burke, T. R., Jr. (1995) *Biochem. J.* 311, 1025–1031.
- Kraulis, P. (1991) *J. Appl. Crystallogr.* 24, 946–950.
- Lam, P. Y., Jadhav, P. K., Eyermann, C. J., Hodge, C. N., Ru, Y., Bachelier, L. T., Meek, J. L., Otto, M. J., Rayner, M. M., Wong, Y. N., et al. (1994) *Science* 263, 380–384.
- Miski, M., Shen, X., Cooper, R., Gillum, A. M., Fisher, D. K., Miller, R. W., & Higgins, T. J. (1995) *Bioorg. Med. Chem. Lett.* 5, 1519–1522.
- Otwinowski, Z. (1993) in *Data Collection and Processing* (Sawyer, L., Isaacs, N., & Bailey, S., Eds.) pp 56–62, SERC Daresbury Laboratory, Warrington, U.K.
- Posner, B. I., Faure, R., Burgess, J. W., Bevan, A. P., Lachance, D., Zhangsun, G. Y., Fantus, I. G., Ng, J. B., Hall, D. A., Lum, B. S., & Shaver, A. (1994) *J. Biol. Chem.* 269, 4596–4604.
- Smyth, M. S., & Burke, T. R., Jr. (1994) *Tetrahedron Lett.* 35, 551–554.
- Smyth, M. S., Ford, H., Jr., & Burke, T. R., Jr. (1992) *Tetrahedron Lett.* 33, 4137–4140.
- Stone, R. L., & Dixon, J. E. (1994) *J. Biol. Chem.* 269, 31323–31326.
- Sun, H., & Tonks, N. K. (1994) *Trends Biochem. Sci.* 19, 480–485.
- Wang, Q. P., Dechert, U., Jirik, F., & Withers, S. G. (1994) *Biochem. Biophys. Res. Commun.* 200, 577–583.
- Watanabe, H., Nakai, M., Komazawa, K., & Sakurai, H. (1994) *J. Med. Chem.* 37, 876–877.
- Wrobel, J., & Dietrich, A. (1993) *Tetrahedron Lett.* 34, 3543–3546.
- Ye, B., & Burke, T. R., Jr. (1996) *Tetrahedron* 52, 9963–9970.
- Zhang, Z. Y. (1995) *J. Biol. Chem.* 270, 11199–11204.
- Zhang, Z. Y., & Dixon, J. E. (1994) *Adv. Enzymol.* 68, 1–36.
- Zhang, Z. Y., Maclean, D., Mcnamara, D. J., Sawyer, T. K., & Dixon, J. E. (1994) *Biochemistry* 33, 2285–2290.

BI961256D